
Hybrid Models for 3D Analysis of Plain and Reinforced Concrete

Using Merlin

Eric Hansen, Victor Saouma

*Department of Civil Engineering
University of Colorado, Boulder
saouma@civil.colorado.edu*

ABSTRACT. This paper reports on the 3D nonlinear analysis of EDF's Benchmark study of four test problems. Analysis is performed through an in-house developed code, Merlin, which combines continuum and localized non-linearities (smeared and discrete cracks).

RÉSUMÉ. summary in french

KEYWORDS: Fracture Mechanics, Finite Element

MOTS-CLÉS : mécanique de la rupture, éléments finis

1. Merlin Description

In general, a non-linear analysis of a reinforced concrete structure may consider the effects of plasticity, and/or damage (distributed failure), and/or fracture (localized, discrete failure).

Merlin combines plasticity with fracture mechanics as two concurrent models. Plasticity-Continuum formulation is best suited to model distributed compressive failure, even through simple Drucker-Prager formulation. Its ability to model tensile failure, through a Rankine-type crack model, is adequate only if extensive cracking is present. On the other hand, a Fracture Mechanics-localized formulation is by far best suited to model individual cracks. This combination allows analyses of concrete structures which consider compressive failure (governed by plasticity), and both distributed failure (by smeared cracking) and localized failure (by fracture) under tension.

Hence, whereas the computational community is still searching for a “universal” model capable of correctly and efficiently predicting the non-linear response of reinforced concrete structures, an attempt is hereby made to combine different models into a single hybrid finite element code. Through this multi-faceted approach, we seek to adopt the right (but not necessarily the best) methodology for the right problem.

Merlin is a 3D static/dynamic finite element code supporting well over 20 different element types, 12 constitutive models, and various nonlinear algorithms. Originally developed for the fracture analysis of dams, it has recently been extended to include reinforced concrete. It supports both discrete cracks, [CER 98] and smeared cracks. Merlin, [REI 97] was originally developed by [REI 93], later extended by [CER 94], and most recently updated and maintained by Cervenka, Hansen and Saouma.

Merlin is only one of a series of programs designed to facilitate its use. KumoNoSu, [HAN 01] is a powerful 3D mesh generator built around the T3D code of [RYP 98] with an easy to use graphical user interface (which makes consultation of the Merlin Manual almost redundant). Spider [HAU 02] is a 3D general purpose finite element postprocessor. RealViewer is a real time display of deformed mesh for each (time or load) increment while Merlin is running. Finally, Cracker, builds on the technology of Kumo to automate the process of (discrete) crack propagation. Whenever Merlin senses that a discrete crack needs to extend branch or nucleate (based on either LEFM or NLFM criterion), analysis is interrupted and control is passed to Cracker. This code in turns will modify the boundary description, generate a mesh and will then restart Merlin (for a full incremental analysis). Presently, the code is fully automated for 2D problems, extension to 3D is currently under development.

1.1. Numerical Models

There are three constitutive models concurrently activated in our code. Two for distributed failures implemented in the spirit of plasticity, [CER 99], and one for localized failure implemented in the spirit of “Fracture Mechanics”, [CER 98].

The continuum has a plasticity based formulation where under tension, Rankine's criteria for concrete (smeared) cracking is adopted:

$$F_i^f = \sigma_{ii}^t - f_{ti}' \leq 0 \quad [1]$$

whereas for compression we use either Drucker-Prager's model [DRU 52], where the failure criteria is given by

$$F_{DP}^P = \alpha \mathbf{I}_1 + \sqrt{J_2} - k = 0 \quad [2]$$

and \mathbf{I}_1 , and J_2 are the first stress tensor invariant, and the second deviatoric stress tensor invariant respectively. α and k are parameters controlling the surface. k controls the hardening/softening and is selected in such a way that the surface at the peak passes through the uniaxial compressive strength

$$k = k^0 \frac{f_c'(\varepsilon_{eq}^p)}{f_c'} \quad [3]$$

or Menétrey-Willam, which is a three parameters models, [MEN 95] which provides more flexibility than the previous model

$$F_{MW}^P = \left[\sqrt{1.5} \frac{\rho}{f_c'} \right]^2 + m \left[\frac{\rho}{\sqrt{6} f_c'} r(\theta, e) + \frac{\xi}{\sqrt{3} f_c'} \right] - c = 0 \quad [4]$$

where

$$m = \sqrt{3} \frac{f_c'^2 - f_t'^2}{f_c' f_t'} \frac{e}{e + 1} \quad [5]$$

$$r(\theta, e) = \frac{4(1 - e^2) \cos^2 \theta + (2e - 1)^2}{2(1 - e^2) \cos \theta + (2e - 1) \sqrt{4(1 - e^2) \cos^2 \theta + 5e^2 - 4e}} \quad [6]$$

where (r, ξ, θ) constitute the Heigh-Westerggard coordinates, f_c' and f_t' are the uniaxial compressive and tensile strength respectively. The curvature of the failure surface is controlled by $e \in \langle 0.5, 1.0 \rangle$ (sharp corner for $e = 0.5$, and circular for $e = 1.0$).

Plastic potential is given by

$$G^p(\sigma_{ij}) = \beta \frac{1}{\sqrt{3}} \mathbf{I}_1 + \sqrt{s J_2} \quad [7]$$

where β determines the return direction. Thus the plastic model is non-associated except for the special case of Drucker-Prager when $\beta = \alpha \sqrt{6}$.

The localized failure model is based on a special interface element, by a failure function:

$$F = (\tau_1^2 + \tau_2^2) - 2c \tan(\phi_f)(\sigma_t - \sigma) - \tan^2(\phi_f)(\sigma^2 - \sigma_t^2) = 0 \quad [8]$$

where: c is the cohesion, ϕ_f is the angle of friction, σ_t is the tensile strength of the interface, τ_1 and τ_2 are the two tangential components of the interface traction vector, and σ is the normal traction component.

The evolution of the failure function is based on a softening parameter u^{ieff} which is the norm of the inelastic displacement vector \mathbf{u}^i . The inelastic displacement vector is obtained by decomposition of the displacement vector \mathbf{u} into an elastic part \mathbf{u}^e and an inelastic part \mathbf{u}^i . The inelastic part can subsequently be decomposed into plastic (i.e. irreversible) displacements \mathbf{u}^p and fracturing displacements \mathbf{u}^f . The plastic displacements are assumed to be caused by friction between crack surfaces and the fracturing displacements by the formation of microcracks.

$$\begin{aligned} F &= F(c, \sigma_t, \phi_f), \quad c = c(u^{\text{ieff}}), \quad \sigma_t = \sigma_t(u^{\text{ieff}}) \\ \mathbf{u} &= \mathbf{u}^e + \mathbf{u}^i, \quad \mathbf{u}^i = \mathbf{u}^p + \mathbf{u}^f \\ u^{\text{ieff}} &= \|\mathbf{u}^i\| = (u_x^i{}^2 + u_y^i{}^2 + u_z^i{}^2)^{1/2} \end{aligned} \quad [9]$$

In this work both linear and bilinear relationship are used for $c(u^{\text{ieff}})$ and $\sigma_t(u^{\text{ieff}})$. in terms of G_F^I and G_F^{IIa} which are the mode I and II fracture energies.

1.2. Algorithmic implementation

Following the previous formulations for plasticity, smeared crack, and discrete cracking, a nonlinear analysis of a concrete structure combines three failure functions:

$$\left\{ \begin{array}{l} \text{Smeared} \left\{ \begin{array}{l} \text{Plasticity} \quad F^p(\sigma_{ij}^{n-1} + E_{ijkl}(\Delta\varepsilon_{kl}^f - \Delta\varepsilon_{kl}^p)) \leq 0 \\ \text{Fracture} \quad F^f(\sigma_{ij}^{n-1} + E_{ijkl}(\Delta\varepsilon_{kl}^p - \Delta\varepsilon_{kl}^f)) \leq 0 \end{array} \right. \\ \text{Discrete} \quad F(\sigma_n + \mathbf{E}\Delta\mathbf{u}_n - \Delta\lambda\mathbf{E}\mathbf{m}, \mathbf{u}_i^{eff}) \leq 0 \end{array} \right. \quad [10]$$

Note that coupling only exists in the smeared crack model between the plasticity (Drucker-Prager or Menétrey-Willam) function and the Rankine smeared crack function. The complete smeared crack model and the discrete crack model remain uncoupled.

Solution of the smeared crack model involves the simultaneous solution of two failure functions, accomplished by:

- 1) $F^p(\sigma_{ij}^{n-1} + E_{ijkl}(\Delta\varepsilon_{kl} - \Delta\varepsilon_{kl}^{f(i-1)} + b\Delta\varepsilon_{kl}^{cor(i-1)} - \Delta\varepsilon_{kl}^{p(i)})) \leq 0$, solve for $\Delta\varepsilon_{kl}^{p(i)}$
- 2) $F^f(\sigma_{ij}^{n-1} + E_{ijkl}(\Delta\varepsilon_{kl} - \Delta\varepsilon_{kl}^{p(i-1)} - \Delta\varepsilon_{kl}^{f(i)})) \leq 0$, solve for $\Delta\varepsilon_{kl}^{f(i)}$
- 3) $\Delta\varepsilon_{kl}^{cor(i)} = \Delta\varepsilon_{kl}^{f(i)} - \Delta\varepsilon_{kl}^{f(i-1)}$

where b is an iteration correction or relaxation factor which can accelerate convergence. As the discrete cracking formulation is separate from the smeared crack, it is solved independently.

2. Test A: Uniaxial Stress Cyclic Load

Fig. 1(a) illustrates the normal stress versus normal strain, while Fig. 1(b) shows the normal stress versus volumetric strain results. The smeared crack/plasticity model

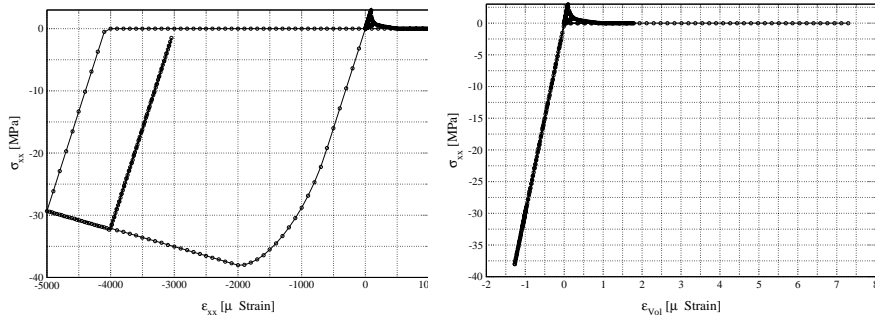


Figure 1. Test A; (a) Normal Strain versus Normal Stress, (b) Normal Stress versus Volumetric Strain

applied to this problem considers non-linear behavior in tension due to material degradation represented by the smeared cracking model, while non-linear behavior in compression is due to plastic behavior. Given these constraints, the model performs quite well in this cyclic tension/compression test. Loading in tension occurs linearly up to the peak tensile strength f'_t , at which point elastic degradation due to smeared cracking causes softening. Unloading occurs at the current secant stiffness back to zero, at which point the material loads elastically in compression, with the stiffness recovery assumed to be due to the closing of the cracks opened during the tensile phase. Plasticity controls the response in the compression regime, and so the material undergoes non-linear hardening up to peak, followed by a more ductile softening response post-peak. Unloading in compression occurs at the elastic stiffness, following the guidelines of plasticity.

When compared with other submissions, Merlin model fits quite well. The only apparent faults are the lack of some permanent displacement in the tensile direction (unloading somewhere between the elastic stiffness and the secant stiffness), and the lack of stiffness degradation in the compressive regime due to compressive cracking. However, considering the limitations of smeared cracking and plasticity theories to capture these respective phenomena, the response of the Merlin analysis is reasonable.

3. Test B: Rotation of Principal Stresses

Again the Drucker-Prager/Rankine model of Merlin was used.

Results are illustrated by Fig. 2 to 3 which illustrate the normal, transversal and shear strains versus their corresponding stresses. The normal stress/strain plot of Fig.

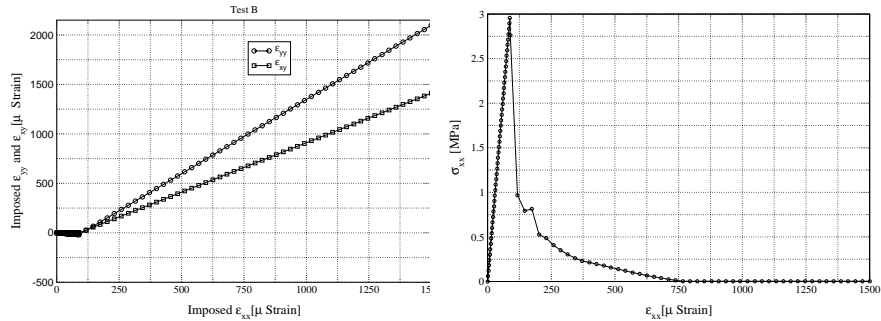


Figure 2. Test B; (a) Load Path, (b) Normal Strain versus Normal Stress

2(b) shows a linear response up to the peak tensile strength f'_t , followed by rapid softening. However, the softening response in the post-peak regime is interrupted by a short plateau near the $125.E - 6$ strain point. Past this plateau, softening continues down to the zero stress level. This plateau in the normal stress/strain response under the rotating principal stress loading scenario was also displayed by [CAR 01] in the context of their “pseudo-Rankine” anisotropic damage formulation, and also by [HAN 00] in the context of his two-surface anisotropic damage/plasticity formulation. Hansen notes that the inflection point at the end of this stress plateau corresponds to a state of biaxial damage. In the case of the Rankine smeared crack model applied in this analysis, the normal stress plateau could also correspond to a state of distributed cracking in two orthogonal directions.

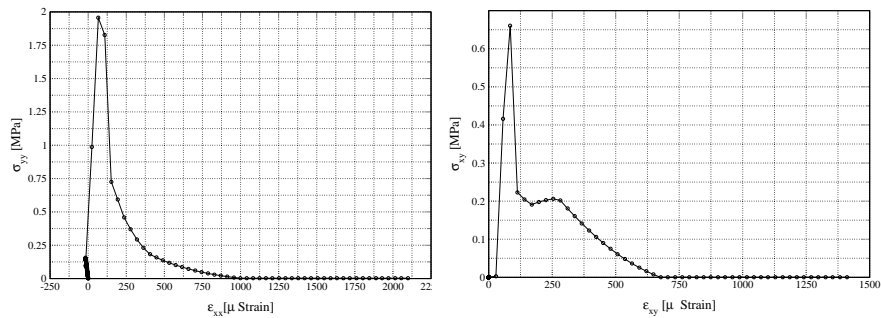


Figure 3. Test B; (a) Transversal Strain versus Transversal Stress, (b) Shear Strain versus Shear Stress

The transversal stress/strain plot of Fig. 3(a) also exhibits an initial linear response up to a peak stress below f'_t , followed by a rapid softening response down to zero stress. This lowered peak strength in the σ_{yy} direction is due to the cracking already present in the σ_{xx} direction. Similar results are shown in the σ_{xy} direction (Fig. 3(b)), with an initial linear response up to a lower shear strength (in comparison to σ_{xx} and σ_{yy}), with the exception being the presence of another stress plateau in shear. At this plateau, the shear stress actually increases slightly before continuing to decrease down to zero.

4. Test C: Reinforced Concrete Beam

This third test seeks to assess the program capabilities in analyzing reinforced concrete structures. We considered only case C1 without shear reinforcement.

This problem was discretized, as all other ones, as a 3D problem in Merlin. The 3D finite element mesh for this problem (and the boundary description) are shown in Fig. 4. Three analyses were undertaken: 1) Linear continuum, single discrete crack

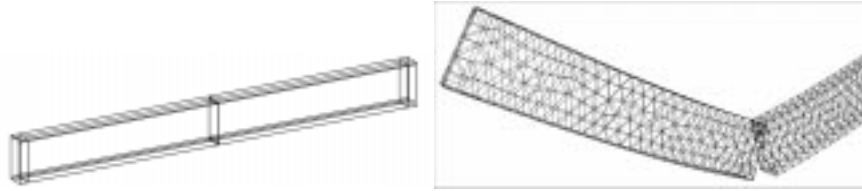


Figure 4. Test C1; Boundary Description and FE (Surface) Mesh

(the single crack was justified by the point load with a localized peak moment); 2) Nonlinear continuum, no discrete crack; and 3) Nonlinear continuum and a single discrete crack. In all cases J_2 plasticity was used for the reinforcement. The mesh for the first and third analyses had 1,263 nodes and 4,748 elements (including 28 interface elements), whereas the mesh without discrete crack had 1,198 nodes and 4,729 elements. In all three cases 200 truss elements were used to model the reinforcement.

Fig. 5 shows the load displacement response for case C1, as well as the steel stress distribution. We observe that the analysis with discrete crack (with ICM element) and linear continuum yields unacceptable results. On the other hand, whereas the analysis with nonlinear continuum is acceptable, it is not as good as the one based on our hybrid approach: discrete crack and nonlinear continuum. This last analysis yielded excellent results, it captured the cracking at 50 kN, prepeak continuous stiffness degradation, and finally the steel hardening up to 3.75 cm of imposed displacement (at which point the analysis was interrupted). However, it should be noted that the full nonlinearity (steel, continuum and crack) necessitated 14 hours of cpu.

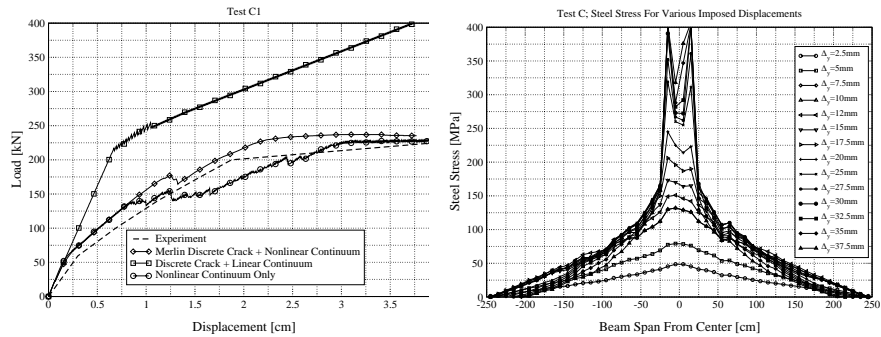


Figure 5. Test C1; Displacement Load Response; Lower Steel Stress Distribution

5. Test D: Mixed Mode Shear Failure

Analysis with Merlin were conducted in two steps. First a 2D analysis with a short initial notch was analysed. Merlin (in conjunction with its companion program Cracker) performed a 2D analysis in which a discrete crack propagation was automatically performed. The analysis proceeded as follows:

- 1) Perform a nonlinear incremental analysis of the specimen containing a short crack.
- 2) If during the analysis, it is determined that the stress at the tip of a crack exceeds the tensile strength, then, Fig. 6:

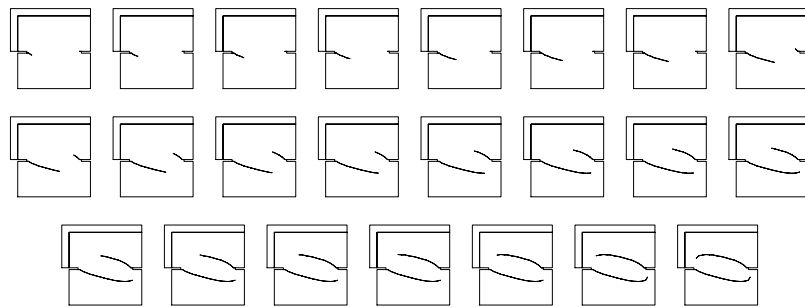


Figure 6. 2D Automated Simulation of Crack Propagation in Tests D

- a) Analysis is interrupted, and direction of crack propagation is passed by Merlin to Cracker.
- b) Cracker will automatically extend the mesh (by a user specified increment), and regenerate a finite element mesh.

c) Control is then transferred to Merlin which restarts the incremental analysis from zero following the remeshing.

3) Analysis will terminate under the following conditions:

a) The last load increment did not result in crack tip stresses exceeding the tensile strength.

b) Crack reaches a surface.

It should be noted that this process is now fully automated in 2D, work is under progress for 3D.

Hence, the analyses for test D was conducted in two parts. First a 2D simulation was performed to obtain the crack trajectory. Upon completion of this analysis, and with the known crack trajectory, the 2D mesh was extruded to a 3D mesh. Finally, the 3D mesh was incrementally analysed with an initial (closed) discrete crack. As the analysis progressed, the crack was automatically “unzipped”, and the crack front progressed, Fig. 7.

The final deformed shape of all tests is shown in Fig. 8. For tests 1a and 1b it is interesting to note that under normal load, the crack extended horizontally first, and when shear was applied, then the cracks kinked accordingly. For tests 2a and 2b, the cracks curved immediately since shear was applied first.

The load displacement curves for all four tests are shown in Fig. 9. Practically all analyses yielded very encouraging results when compared with the experimental results.

Analyses for test D had approximately 3,000 elements, and 1,200 nodes. cpu time for tests 1-a and 1-b was about 11 minutes, and 3.0 minutes for tests 2-a and 2-b.

6. Conclusion

This report has proven the capabilities of Merlin to combine discrete cracking, smeared cracking, and plasticity to model material nonlinearities in the context of a variety of loading scenarios prescribed by EDF. The capability to model discrete cracking through the use of interface elements and nonlinear fracture mechanics (NLFM) allows the simulation of localized cracks in a structure and their effects on the response of that structure. Smeared cracking allows models to capture the overall degradation of the strength and stiffness of a structure due to distributed cracking, and plasticity further complements the analysis capabilities by improving the response predictions of concrete under compressive loading and also the response of steel reinforcing bars. Together, these features allow Merlin to accurately predict the responses of a variety of structures under various loading conditions.

Acknowledgements

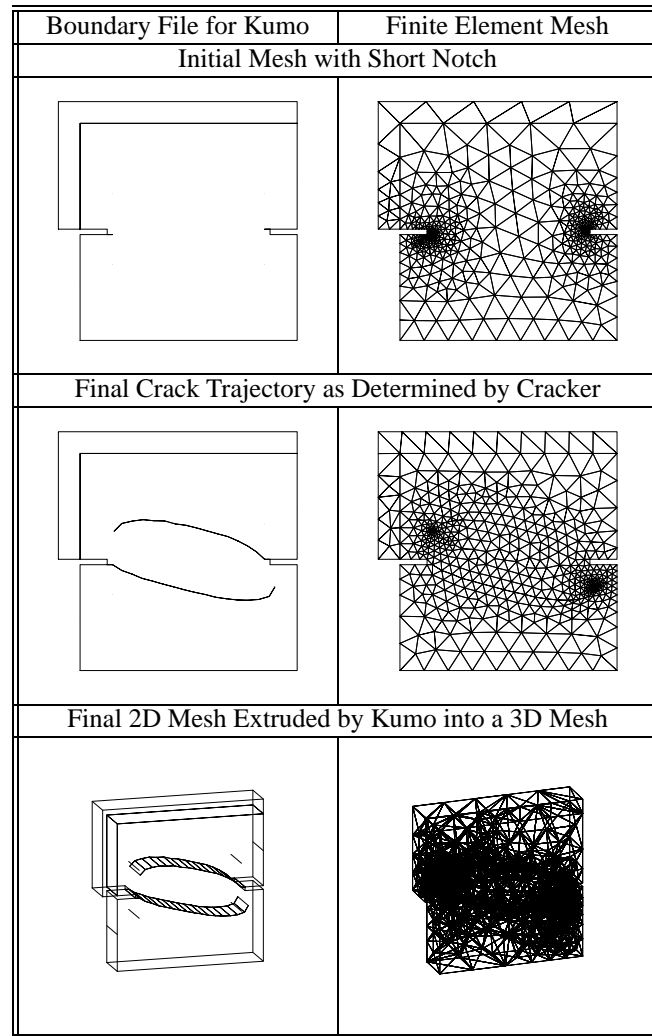


Figure 7. *Simulation of Tests D*

The authors would like to thank, first and foremost, Dr. Jan Červenka for his continuous collaboration in the development of Merlin.

The development of Merlin was originally supported by Mr. Doug Morris and the Electric Power Research Institute (EPRI). The authors would like to thank Mr. Uchita and the Tokyo Electric Power Company (TEPCO), and Mr. Shimpo and the Tokyo Electric Power Services Company (TEPSCO) for their current support of the

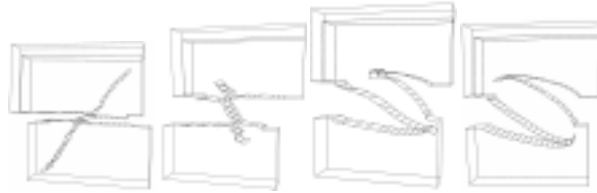


Figure 8. Final Deformed Shapes for Tests D-1a, D-1b, D-2a and D-2b

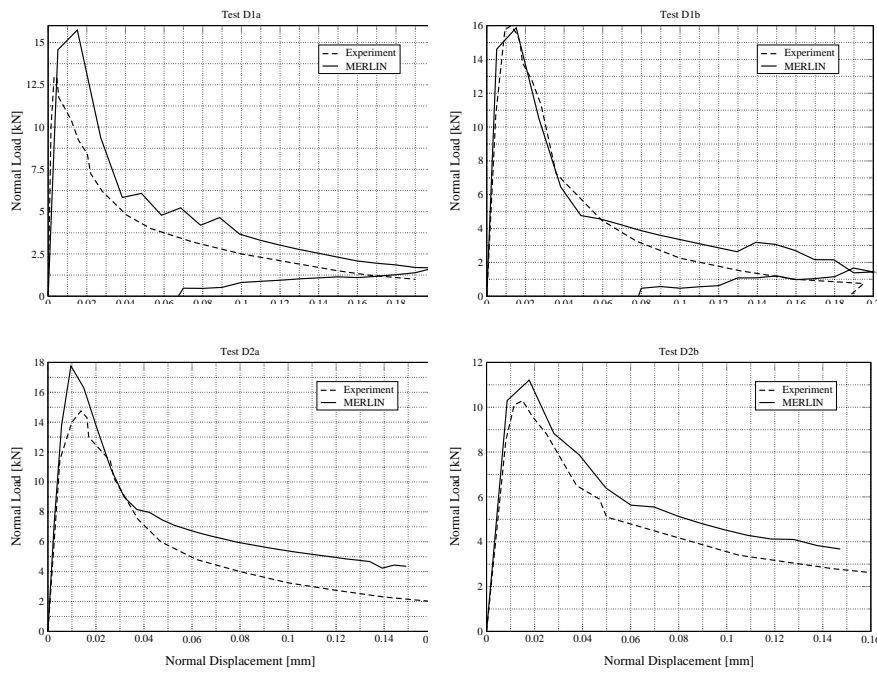


Figure 9. Load Displacement Curves for Tests D-1a, D-1b, D-2a and D-2b

extension of the capabilities of Merlin. Further thanks to Dr. Daniel Ryppl [RYP 98] for the adoption and use of his robust 3D mesh generator T3d.

Finally, Dr. Ben Spencer's is acknowledged for his analysis of EDF's test problems A and B (and an initial unreported 2D analysis of tests D).

7. References

- [CAR 01] CAROL I., RIZZI E., WILLAM K., “On the formulation of anisotropic elastic degradation. Part II: Generalized pseudo-Rankine model for tensile damage”, *International Journal of Solids and Structures*, vol. 38, num. 4, 2001, p. 519–546.
- [CER 94] CERVENKA J., “Discrete Crack Modeling in Concrete Structures”, PhD thesis, University of Colorado, Boulder, December 1994.
- [CER 98] CERVENKA J., CHANDRA KISHEN J., SAOUMA V., “Mixed Mode Fracture of Cementitious Bimaterial Interfaces; Part II: Numerical Simulation”, *Engineering Fracture Mechanics*, vol. 60, num. 1, 1998.
- [CER 99] CERVENKA J., CERVENKA V., “Three Dimensional Combined Fracture-Plastic Material Model for Concrete”, *5th U.S. National Congress on Computational Mechanics*, Boulder, CO, August 1999.
- [DRU 52] DRUCKER D., PRAGER W., “Soil Mechanics and Plastic Analysis of Limit Design”, *Quarterly of Applied Mathematics*, vol. 10, num. 2, 1952, p. 157–165.
- [HAN 00] HANSEN E., “A two-surface anisotropic damage/plasticity model for plain concrete”, PhD thesis, University of Colorado at Boulder, Boulder, CO, December 2000.
- [HAN 01] HANSEN E., SAOUMA V., “KumoNoSu, a 3D Interactive Graphics Mesh Generator for MERLIN”, report, 2001, Report Submitted by the University of Colorado to the Tokyo Electric Power Service Company, <http://civil.colorado.edu/~saouma/Kumo>.
- [HAU 02] HAUSSMAN G., SAOUMA V., “Spider, a 3D Interactive Graphics Finite Element Post-Processor”, report, 2002, Report Submitted by the University of Colorado to the Electric Power Research Institute, Palo Alto, <http://civil.colorado.edu/~saouma/Spider>.
- [MEN 95] MENÉTREY P., WILLAM K., “Triaxial failure Criterion for Concrete and its Generalization”, *ACI Structural Journal*, vol. 92, num. 3, 1995, p. 311–318.
- [REI 93] REICH R., “On the Marriage of Mixed Finite Element Methods and Fracture Mechanics: An Application to Concrete Dams”, PhD thesis, University of Colorado, Boulder, May 1993.
- [REI 97] REICH R., CERVENKA J., SAOUMA V., “MERLIN, A Three-Dimensional Finite Element Program Based on a Mixed-Iterative Solution Strategy for Problems in Elasticity, Plasticity, and Linear and Nonlinear Fracture Mechanics”, report, 1997, EPRI, Palo Alto, <http://civil.colorado.edu/~saouma/Merlin>.
- [RYP 98] RYPL D., “Sequential and Parallel Generation of Unstructured 3D Meshes”, PhD thesis, Czech Technical University in Prague, 1998, <http://ksm.fsv.cvut.cz/~dr/t3d.html>.